IMPACT: International Journal of Research in Engineering & Technology (IMPACT: IJRET)
ISSN(E): 2321-8843; ISSN(P): 2347-4599
Vol. 2, Issue 11, Nov 2014, 7-18

ENERGY QUALITY IMPROVEMENT USING AN ADVANCED CONTROL STRATEGY BASED TRANSFORMERLESS SHUNT HYBRID POWER FILTER

MUSTAPHA SARRA[1], JEAN-PAUL GAUBERT[2], KAMAL DJAZIA[3] & FATEH KRIM[4]

[1]Department of Electronics, University of Bordj Bou Arreridj, El Anasser Ex Galbois, Algeria

[2]Laboratoire d'Informatique et d'Automatique Pour Les Systèmes (LIAS), University of Poitiers, Poitiers, France

[3]Department of Electronics, University of M'sila, Algeria

[4]Department of Electronics, University of Setif, Algeria

ABSTRACT

A Shunt Hybrid Active Power Filter (SHAPF) is proposed in this paper in order to enhance the power quality and compensate reactive power required by nonlinear load. The advanced control algorithm applied to the SHAPF in based on a Multi-Variable Filters (MFV) combined with a robust PLL to determine the reference current. The SHAPF is formed by a single 7^{th} tuned LC filter per phase and a small-rated three-phase active filter, which are directly connected in series without any matching transformer. Proposed topology provides significant inverter power rating reduction. The required rating of the active filter is much smaller than that of a conventional standalone active filter be. All simulations are performed by using Matlab-Simulink Power System Blockset and validated with an experimental test bench developed in the LIAS laboratory, University of Poitiers. Various simulation and experimental results of the proposed control algorithm are presented under steady state and transient conditions to confirm his validity and effectiveness.

KEYWORDS: Energy Quality, Harmonics, Multi-Variable Filter (MVF), Phase Looked Loop (PLL), Shunt Hybrid Active Power Filter, Voltage Source Inverters

INTRODUCTION

For some years growing use of non-linear loads, like diode rectifiers, ovens, telecommunication power supplies, causes exorbitant neutral currents, harmonic current injection and develops non-sinusoidal currents from utility networks, thereby contributing of power quality deterioration in power distribution networks or industrial power systems. They lead in bad power factor, lower effectiveness and interference to adjacent communication systems. Traditionally based passive filters (PFs) were used to suppress current harmonics and enhance power factor. However, these PFs have the disadvantages of fixed compensation, bulkiness and occurrence of resonance with other elements.

To dominate the above mentioned disadvantages inherent in PFs, various type of pure active power filters (APF) configuration have been developed; however they also have some drawbacks such as:

- Difficulty to build a large-rated current source.
- High cost of active filters limits their application in industrial power systems. [1]-[7].
- To minimize the problems and to achieve benefits of PFs and pure APFs, different topologies of hybrid active filters by connecting APFs and PPFs in series or parallel with various control strategies, were proposed in recent

years as lower cost alternatives to pure APFs used alone. This paper presents a transformerless SHAPF composed by a single LC filter per phase tuned to the seventh-harmonic frequency and a small-rated three-phase active filter based on a three-phase voltage-source PWM converter. The passive and active filters are directly linked in series. The DC voltage of the active filter is much lower than the supply line-to-line RMS voltage because no supply voltage is applied through the active filter. The supply voltage is applied across the capacitor of the passive filter. Furthermore, no additional switching-ripple filter is intended for the SHAPF because the LC filter operates not only as a harmonic filter but also as a switching-ripple. This SHAPF is based on advanced control algorithm using a Multi-Variable Filters (MFV) combined with a robust PLL to determine the reference current for the algorithm control [8]-[11].

SHAPF TOPOLOGY AND PRINCIPLE OF COMPENSATION

Figure 1 presents the power scheme of the proposed SHAPF designed in order to reduce the total harmonic distortion (THD) of current source i_s below 5%. The SHAPF is composed of a three-phase three wire supply voltage, three phase six pulse rectifier, and the active filter which is directly connected to the system through the LC filter. The passive filter proposed in this topology is not tuned to most dominant 5th harmonic frequency but the second most dominant 7th harmonic frequency for the following reasons:

- Passive filter tuned to the 7th harmonic frequency is less bulky and less expensive than that tuned to 5th frequency as long as both filters have the same inductor L_F.
- The passive filter tuned to the 7th harmonic frequency offers less impedance to the 11th and 13th harmonic components, compared to that tuned to the 5th harmonic frequency.

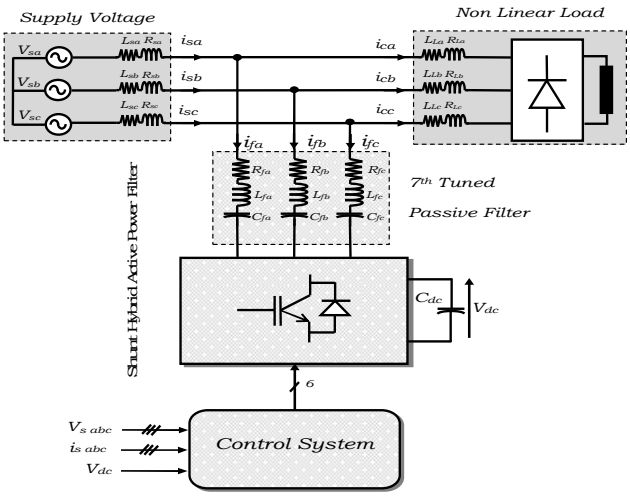

Figure 1: Topology of the Proposed SHAPF

This hybrid filter topology predicts important inverter power rating reduction and permits the inverter to have a reduced DC-side voltage. The passive filter absorbs the 7th harmonic current, while the active filter compensates the other harmonic currents produced by the non linear load by injecting equal but opposite harmonic compensating current.

Figure 1 can be streamlined for one phase as shown in Figure 2(a), where *Zs* is the source impedance and Z_F is the passive filter total impedance. The active filter is inspected as a voltage source V_{AF}, the load is supposed to be an ideal

current source I_L. When the active filter is not connected (V_{AF} =0), assuming that the supply voltage is balanced and sinusoidal gives the supply harmonic current I_{Sh} as follows:

$$I_{Sh} = \frac{Z_F}{S.L_S + Z_F} I_{Lh} \quad (1)$$

If the supply impedance $\omega_h L_S$ is much smaller than Z_f, desirable filtering characteristics could not be obtained. Furthermore, harmonic resonance between L_S and Z_F may arise at a specific frequency, thus producing the so-called harmonic-amplifying phenomena.

When the active filter is connected, it helps the passive filter to sink the load harmonic current I_{Lh}, so that a small amount of harmonic current can flow to the supply. Moreover, the active filter can damp out the harmonic resonance. The supply harmonic current I_{Sh}, the terminal harmonic voltage V_{Th}, and the output voltage of the active filter V_{AF} are given as follows:

$$I_{Sh} = \frac{Z_F}{R + S.L_S + Z_F} I_{Lh} \quad (2)$$

$$V_{Th} = -\frac{S.L_S Z_F}{R + S.L_S + Z_F} I_{Lh} \quad (3)$$

$$V_{AF} = \frac{Z_F}{R + S.L_S + Z_F} I_{Lh} \quad (4)$$

Equation (2) indicates that Figure 2(a) is equivalent in I_{Sh} to Figure 2(b). This means that a pure resistor K (Ω) is placed in series with L_S as shown in Figure 2(b). If $K \gg Z_F$ all the harmonic currents injected from the load would sink into the *LC* filter. If $K \gg \omega_h L_S$, *K* would dominate the filtering characteristics. In addition K behaves as a resistor to damp out parallel harmonic resonance between L_S and Z_F. Briefly, the principle is to increase Z_S and decrease Z_F simultaneously. [8] - [10]

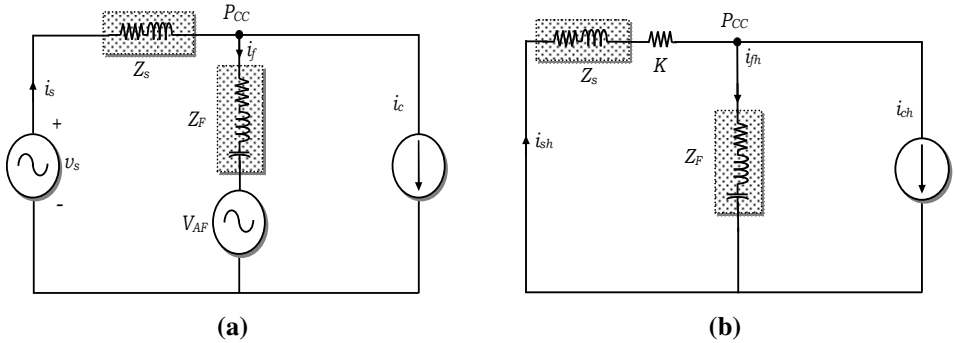

Figure 2: Single Phase Equivalent Circuit

Figure 3 presents the filtering characteristics (relationship between I_{Sh} and I_{Lh}) of the SHAPF for different values of *K*. When the active power filter is not connected in series with the passive *LC* filter, harmonic-amplifying phenomenon appears in a frequency range of 200–700 Hz. When the active power filter is linked, no harmonic-amplifying phenomenon happens. Furthermore, the filtering characteristic of the SHAPF is satisfying only at the seventh harmonic frequency.

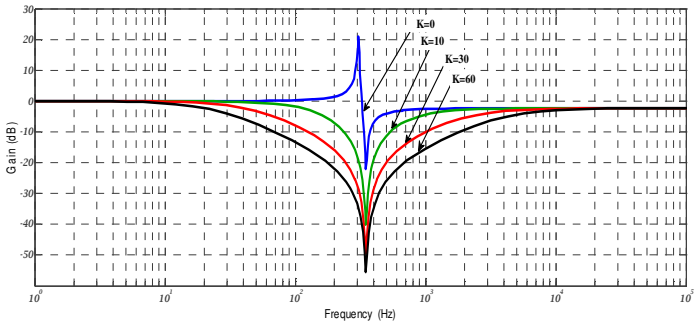

Figure 3: Filtering Characteristics

Hybrid Active Filter Control

The proposed SHAPF control scheme is presented in Figure 4, which detects the three-phase supply currents Is_{abc}, three-phase voltage supply Vs_{abc} and the DC-bus voltage V_{dc} and then builds the reference voltages Vs_{abc}^{*} for the PWM voltage source inverter. At first, the three-phase supply currents (I_{sa}, I_{sb}, and I_{sc}) are measured and transformed into the instantaneous active (I_d) reactive (I_q) components using synchronous reference frame (SRF) rotating at fundamental angular speed with the positive sequence of the system voltage (5).

$$\begin{bmatrix} i_d \\ i_q \end{bmatrix} = \frac{2}{3}\begin{bmatrix} \cos\hat{\theta} & \cos\left(\hat{\theta}-\frac{2\pi}{3}\right) & \cos\left(\hat{\theta}+\frac{2\pi}{3}\right) \\ -\sin\hat{\theta} & -\sin\left(\hat{\theta}-\frac{2\pi}{3}\right) & -\sin\left(\hat{\theta}+\frac{2\pi}{3}\right) \end{bmatrix}\begin{bmatrix} i_{s_a} \\ i_{s_b} \\ i_{s_c} \end{bmatrix} \tag{5}$$

Where $\hat{\theta}$ represents the positive sequence phase of the system voltage which is provided by the robust PLL. The system under study is a three-wire system where the zero sequence may be neglected, so only i_d and i_q are considered. The active and reactive currents can also be decomposed in their DC and AC components.

$$\begin{bmatrix} i_d \\ i_q \end{bmatrix} = \begin{bmatrix} i_{d_{DC}} + i_{d_{AC}} \\ i_{q_{DC}} + i_{q_{DC}} \end{bmatrix} \tag{6}$$

Where $(i_{d_{DC}}, i_{d_{qDC}})$ are respectively the d-axis and q-axis direct components which correspond respectively to the fundamental active and reactive components, and $(i_{d_{AC}}, i_{d_{qAC}})$ are respectively the d-axis and q-axis alternating components which correspond respectively to the harmonic active and reactive components.

It is hoped that the network supplies the DC values of the active current, while its AC components, as well as the reactive current, is supplied by the SHAPF. Concerning the reactive current, its DC value is provided by the passive filter, while the inverter provides an AC voltage to damp the harmonics. A second-order low-pass filter (LPF) with a cutoff frequency of 12 Hz extracts AC components $\tilde{i}_d$ from i_d. The obtained $\tilde{i}_d$ and i_q^{*} are then fed into the proportional plus integral (PI) regulators to generate the required voltage command for the inverter. A *dq* to *abc* transformation is applied to convert the inverter voltage command back to three-phase quantities. The sine/triangle modulation generates square wave switching commands to achieve harmonic isolation and DC-bus power balancing of the active filter inverter.

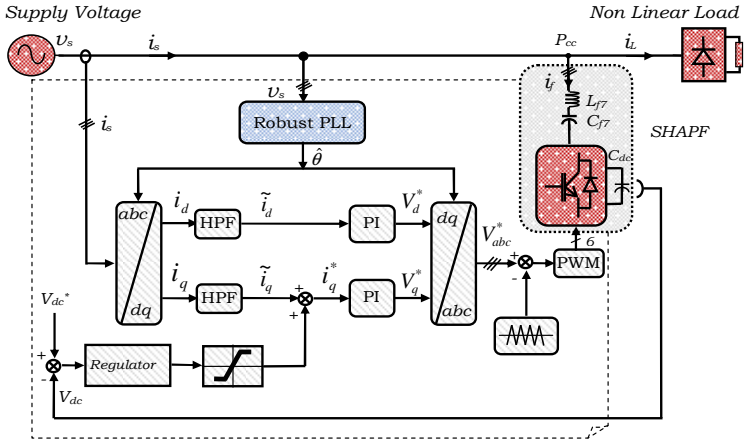

Figure 4: The SHAPF Control Diagram

DC-Bus Voltage Control

The SHAPF can achieve and control automatically the DC capacitor voltage by itself without any external power supply. Figure 5 describes the scheme of the DC-voltage control with a proportional-integral (PI) regulator. When the SHAPF is inspected to generate a fundamental voltage in phase with the fundamental current of the passive filter, an active power formed by the main current and the fundamental voltage is provided to the DC capacitor. Therefore, the electrical quantity to be controlled in a DC voltage feedback loop is not ΔId but ΔIq [8].

Given that the current control buckle (inner buckle) must be faster than the DC voltage buckle (external buckle) at high switching frequency, which indicates that the bandwidth of the external buckle is much lower than that of the inner one, then it can be supposed that the poles of its transfer function is not concerned in the external buckle stability. Thus, in steady state the current closed buckle gain has a unity value (I_s (s)/I_s^*(s) =1). Then, the global control buckle scheme in Figure 5(a) can be simplified. Consequently, the choice of PI parameters (K_i, K_p) is based on the step response of this simplified closed buckle. Otherwise, to limit and sleek supply current at started and dumping transient time, an Antiwindup loop has been combined to the PI controller (Voltage regulator) as shown in Figure 5(b).

Then, the expression of voltage control buckle is:

$$\frac{V_{dc}^*}{V_{dc}} = \frac{\frac{K_p}{C_{dc}}.S + \frac{K_i}{C_{dc}}}{S^2 + \frac{K_p}{C_{dc}}.S + \frac{K_i}{C_{dc}}} \tag{7}$$

From (5) the relation between V_{dc} and V_{dc}^* is a second order transfer function in the form of:

$$\frac{V_{dc}^*}{V_{dc}} = \frac{2.\xi\omega_n.S + \omega_n^2}{S^2 + 2.\xi\omega_n.S + \omega_n^2} \tag{8}$$

Where ω_n is natural frequency and ξ is coefficient of damping. The transfer function has two poles and one zero, this demonstrates that the proposed voltage controller based on an Antiwindup buckle, assures a fast response and an appropriate stability for transient states. By equaling (5) and (6), K_i and K_p can be deduced. [14, 15].

From where, $K_p = 2.\ \xi.\ \omega_n.C_{dc}$ and $K_i = C_{dc}.\omega_n^2$

Otherwise, the Bode diagram of the closed loop transfer function shown in Figure 5 (c) represents a suitable stability with a margin phase PM=127° and a bandwidth B_W =62 rad

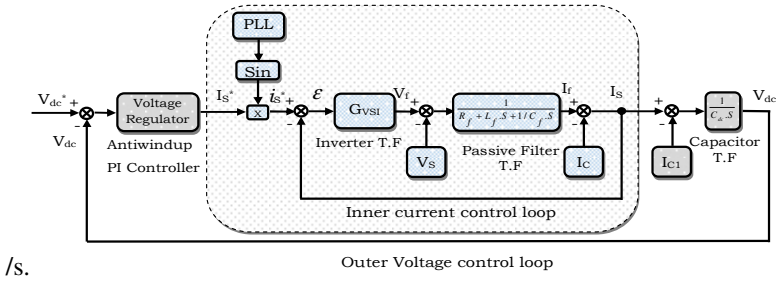

/s.

Figure 5: Block Diagram of the DC-Bus Voltage Control

Proposed Robust PLL

The fundamental objective of the control strategy proposed in this paper is to enhance the performance of the SHAPF by using a robust PLL based on a Multi-Variable Filter (MVF) which can extract directly the fundamental voltage in the α-β axis with high performance that permits making insensible the PLL to the perturbations specifically to the harmonic and unbalanced voltage. [16]-[19].

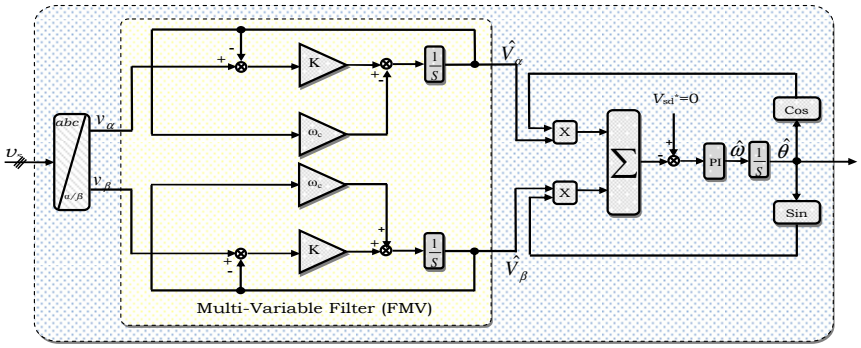

Figure 6: Robust PLL Principle Scheme

Figure 6 illustrates the principle scheme of the proposed robust PLL. The important part of this system is the MVF expressed in (7), that permit filtering the stationary reference frame components of the main voltages at the network frequency (50 Hz), without leading either a phase shift or a voltage change amplitude.(H(s)=0db).

Where, (ω_c, k) are the cut-off frequency and the dynamic gain respectively.

$$\hat{V}_\alpha(s)=\frac{k(s+k)}{(s+k)^2+\omega_c^2}.V_\alpha(s)-\frac{k.\omega_c}{(s+k)^2+\omega_c^2}.V_\beta(s)$$
$$\hat{V}_\beta(s)=\frac{k(s+k)}{(s+k)^2+\omega_c^2}.V_\beta(s)+\frac{k.\omega_c}{(s+k)^2+\omega_c^2}.V_\alpha(s) \quad (7)$$

The bode diagram of the Multi-Variable Filter in 3D results in the following figures:

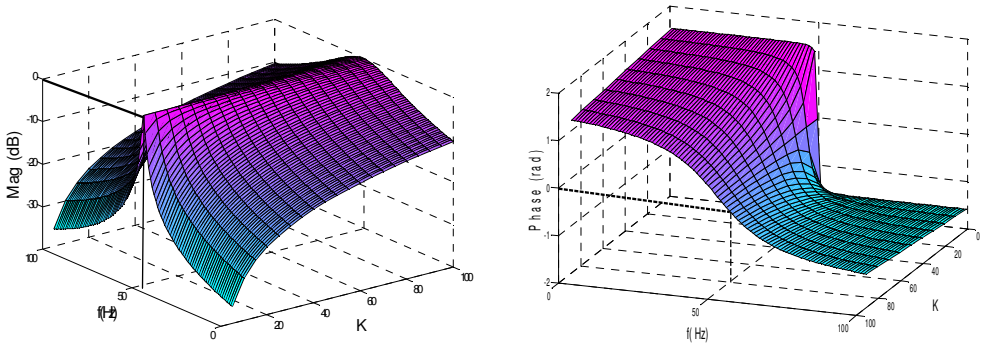

(a) **(b)**

Figure 7: Bode Diagram of Multi-Variable Filter a) Magnitude and b) Phase versus f and K

The Figure 7 indicates that, at 50Hz, the phase angle of bode diagram is null, thus the two input and output signals are in phase. Figure 8 presents the robust PLL simulation results done in the worst events. Figure 8(a) illustrates the contaminated supply voltage containing harmonics and random noise, and in Figure 8(d) is presented the absolute sinusoidal and stable voltage generated by the proposed robust PLL, that demonstrates the perfect results in filtering of the voltage harmonics without generating any phase-shifting and remove the unbalance which can arise in the electrical network.

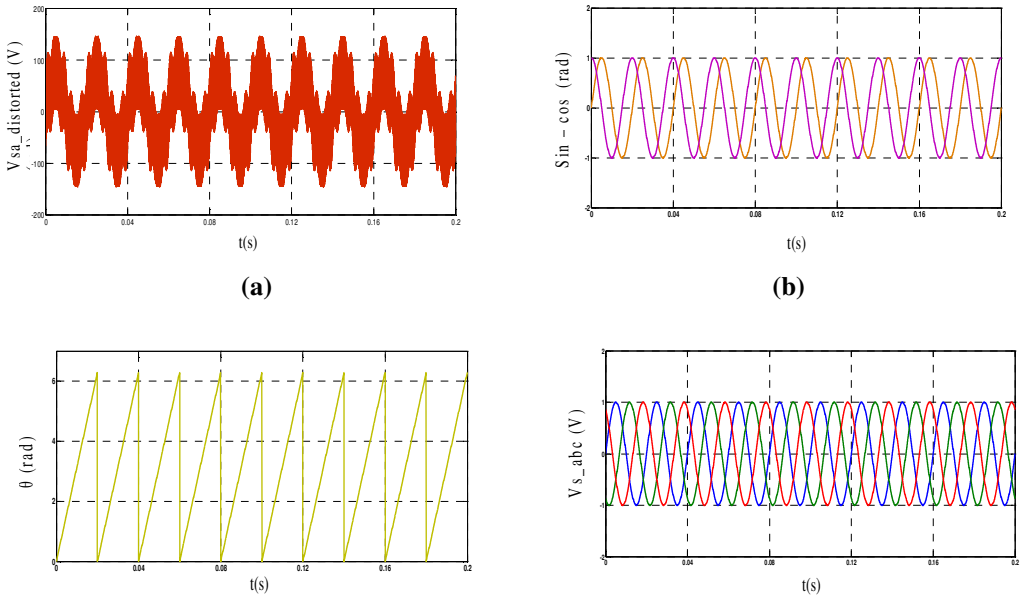

(a) **(b)**

(c) **(d)**

Figure 8: Robust PLL Simulation Results

Modeling and Simulation of the System

To simulate the proposed SHAPF control strategy, a model is developed in Matlab/Simulink® environment using SimPower Systems Blockset. The complete active power filter system is composed mainly of a three-phase source, a nonlinear load which is a three phase rectifier feeding an inductive load, a PWM voltage source inverter, and a control bloc. It is worth mentioning that the simulation parameters are identical to those used for experimentation and are recapitulated in Table 1.

Table 1: System Components and Parameters Values

Supply Voltage	V_{Sabc} = 50V (rms)	Quality Factor Q	42
Line frequency	f =50 Hz	APF DC-capacitor	C_{dc} = 1100 µF
Supply line impedance	R_S=0.1 Ω , L_S =0.05 mH	APF DC-bus voltage	V_{dc}^* = 15 V
Nonlinear load components	R_L=0.1 Ω , L_L=0.05 mH R_{D1}=16.1 Ω , R_{D2} =30 Ω L_D =1 mH	Voltage regulator Parameters	K_{pv}=0.156, K_{iv}=11.1
		Current regulator Parameters	K_{pc}=0.156, K_{ic}=11.1
		Resonant frequency	350 Hz
7th tuned passive filter	L_{F7} =1.9 mH, L_{C7} =110µF	LPF Cut-off frequency	f_{LPF} = 12 Hz

Computer simulation inspects the viability and effectiveness of the proposed SHAPF control strategy. Firstly, the results of simulation before connecting the filter to the network polluted by the nonlinear load are presented in Figure 9. It can be noticed in Figure 9(d) that, without passive ore active filters in the system, the source current i_s presents a high harmonic distortion (THD_i=27, 38%) produced by the presence of the nonlinear load. Otherwise, it can also be noted that the significant current generated by this nonlinear load, are 5th, 7th, 9th and 11th order, among them the biggest is the 5th.

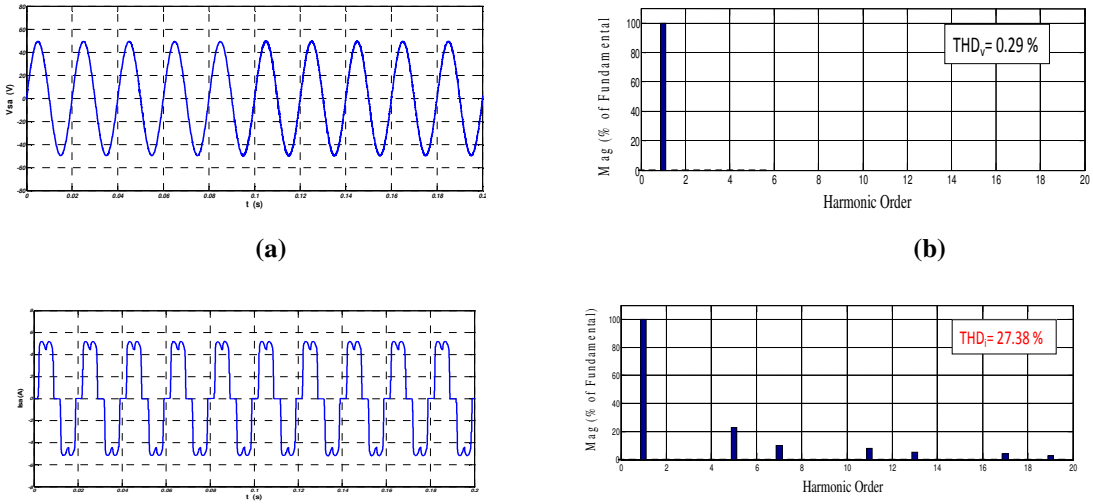

Figure 9: Simulation Waveforms before Connecting the SHAPF

Simulation results of the system are presented in steady and transient states in the next section.

Figure 10 presents the supply voltage waveform V_{sa} *(V),* load current I_{ca} (A), main current I_{sa} (A), the DC-bus voltage V_{dc} *(V).* When the SHAPF is connected to the system (switched on) at time t=0.08s, it can decrease the supply current THD_i from 27.38% to 2.71%. Thus, it becomes almost sinusoidal waveform, which attests that the proposed SHAPF control strategy is able to compensate current harmonics successfully. On the other hand, it can be observed how the SHAPF deal under a first step change in the nonlinear load DC side at t=0.2s from R_{D2} to R_{D1} and from R_{D1} to R_{D2} at t=0.3s. After the nonlinear load changes happened, the main current was deformed for about one cycle (about 20ms), which would not produce any bad effect on external circuits and equipment, because the proposed SHAPF with its robust control strategy recovered from the transient state in one cycle. The DC-bus voltage V_{dc} was well stabilized, even in the

transient state, because of the use of the DC-voltage control with its Antiwindup buckle.

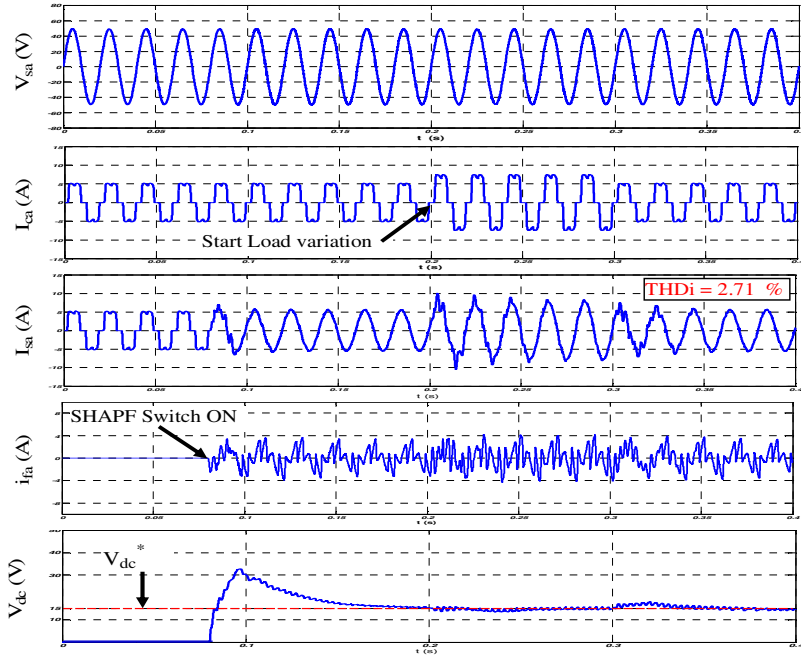

Figure 10: Simulation Waveforms after Connecting the SHAPF in Transient State

EXPERIMENTAL RESULTS

The SHAPF experimental test is done using the test bench developed in the LIAS-ENSIP laboratory, University of Poitiers (Figure 12). The input step-down transformer (20KVA, 400/230 V) is linked to the electrical network. The three-phase shunt active power filter is achieved with a 20 KVA voltage source inverter. This VSI contains a three-phase IGBT 1200 V, 50 A (SKM 50 GB 123D). To ensure the insulation and the dead time of control signals a developed card based on the IXDP630 component and a special driver circuit (SEMIKRON, SKHI 22) is used. The control strategy is implemented using a dSPACE card DS1104 developed under Matlab/Simulink™ RTW environment. The sampling time using in practical tests for the proposed systems is 50 µs [17-19].

Figure 13 (a, b) present the experimental results of the proposed robust PLL with unbalanced and polluted supply voltage, and in Figure 13(c, d), is presented the perfect sinusoidal and balanced voltage generated by the proposed robust PLL. Like simulation results, these experimental results demonstrate the effectiveness of the voltage harmonics filtering without generating any phase-shifting and eliminate the unbalance which can appear in the electrical network. [19]

Figure 11: Photography of the APF System Prototype

The experimental results before connecting the filter to the network polluted by the nonlinear load are presented in Figure 12. Without passive or active filters connected to the system, the source current i_s presents a high harmonic distortion (THD_i = 23%) caused by the presence of the nonlinear load. Otherwise, it can also be noted that the significant current generated by this nonlinear load, are 5th, 7th, 9th and 11th order, among them the biggest is the 5th, that confirm the simulation results. [19]

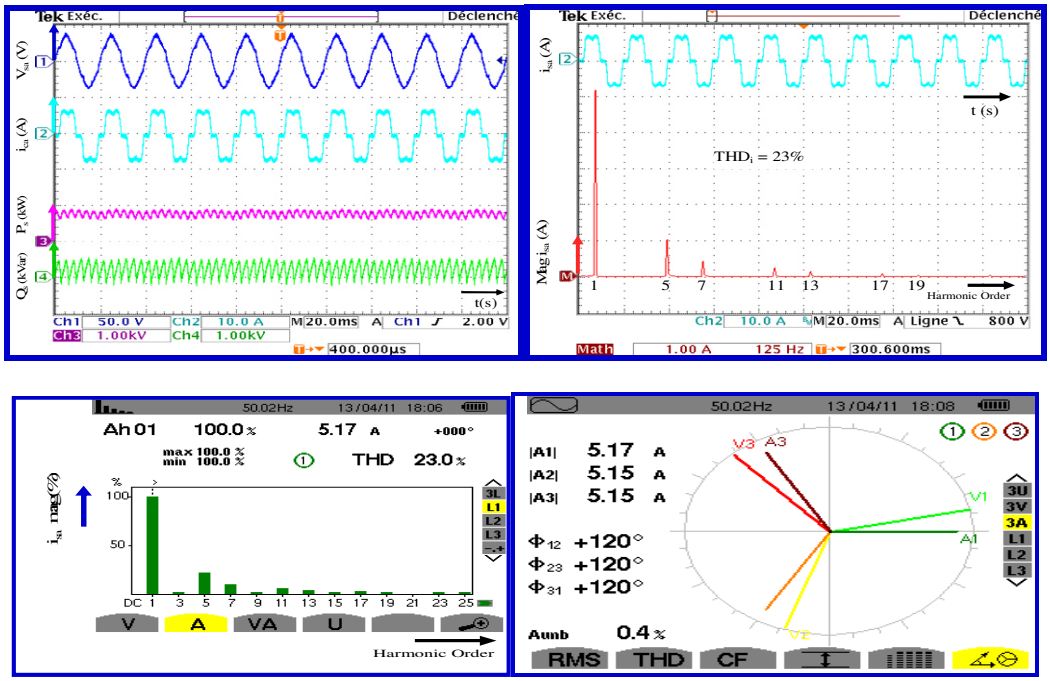

Figure 12: Experimental Waveform before Connection of the SHAPF

The experimental results of the system in steady state are recapitulated in Figure 13. Figure 13(a, b) present the supply voltage waveform V_{sa} *(V),* load current I_{ca} (A), supply current I_{sa} (A), the DC-bus voltage V_{dc} *(V)* regulated at reference value V_{dc}^* fixed at 15V, the active power P (W) and the reactive power Q (VAR). When the SHAPF is applied to the system, it can decrease the supply current THD_i from 27.38% to 3.9% (2.7% in simulation) as it is shown in Figure 16(a, b), so, it becomes almost sinusoidal waveform, which demonstrates that the proposed SHAPF control strategy has the capability of compensating for current harmonics successfully. The DC-bus voltage V_{dc} was well regulated, even in the transient state, because of the use of the DC-voltage control with its Antiwindup loop.

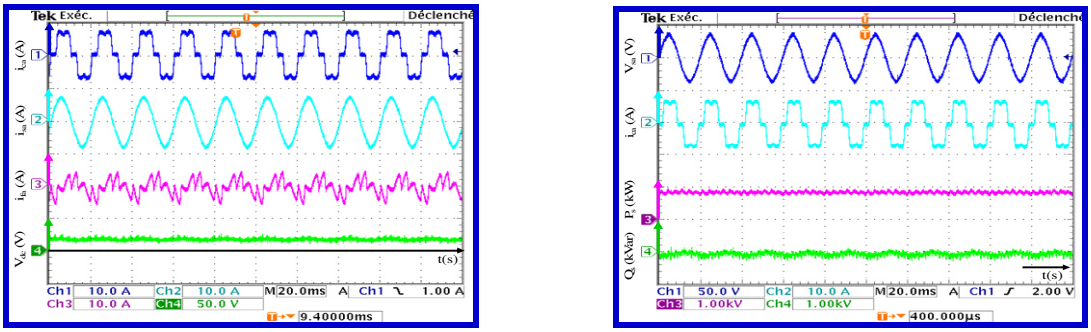

(a) **(b)**

Figure 13: Experimental Waveform after Connection of the SHAPF

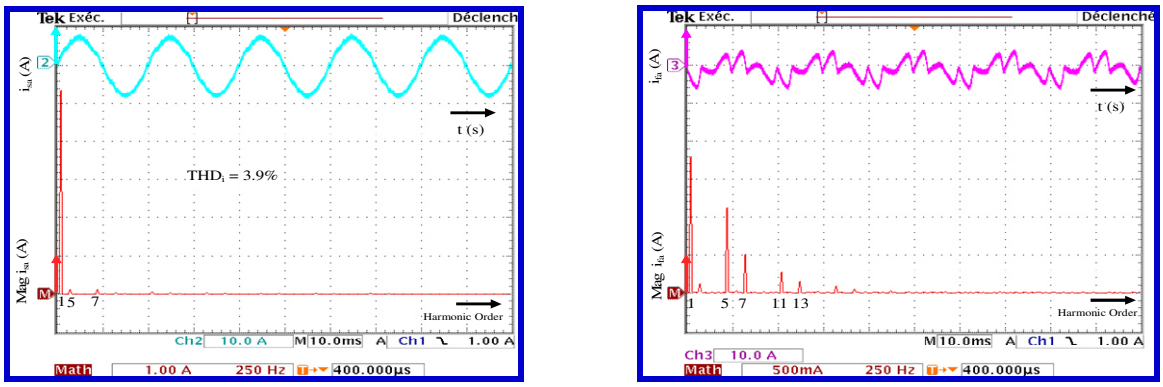

(a) **(b)**

Figure 14: Supply and Compensating Currents with their Spectrums

CONCLUSIONS

A Shunt Hybrid Active Power Filter (SHAPF) has been proposed in this paper, to enhance the power quality and compensate reactive power required by nonlinear load. The control algorithm consisting of synchronous reference frame (SRF) rotating at fundamental angular speed uses a Multi-Variable Filters (MFV) combined with a robust PLL. The proposed SHAPF is formed by a single 7^{th} tuned LC filter per phase and a small-rated three-phase active filter, which are directly connected in series without any matching transformer. The required rating of the active filter is much smaller than that of a conventional standalone active filter. With the advanced control system designed in this paper the proposed SHAPF can attenuate harmonics well and has a good dynamic performance. Finally, various simulation and experimental results of the proposed control algorithm are presented under steady state and transient conditions to confirm his validity and effectiveness.

REFERENCES

1. Akagi H. New trends in active filters for power conditioning. IEEE Trans. Ind. App.1996; 32: 1312–1322.
2. Akagi H, *Kanazwa Y, Nabae N.* Generalized theory of the instantaneous reactive power in three-phase circuit. IPEC'83-International Power Electronics Conference", Tokyo, Japan1983, pp. 1375–1386.
3. Peng F. Z, Akagi H, Nabae A. A study of active power filters using quad series voltage source PWM converters for harmonic compensation, IEEE Trans. Power Electronics, 1990; 5: 9-15.
4. Fujita H, Akagi H. A Practical Approach to Harmonic Compensation in Power Systems-Series Connection of Passive and Active Filters. *IEEE Trans. Ind. App. 1991;* 27, no.6:1020-1025.
5. Fujita H, Akagi H. An approach to harmonic-free ac/dc power conversion for large industrial loads: The integration of a series active filter with a double-series diode rectifier. IEEE Trans. Ind. App.1997; 33: 1233–1240.
6. Bhattacharya S, Cheng P. T, Divan D. M. Hybrid solutions for improving passive filter performance in high power applications. IEEE Trans. Ind. App. 1997; 33:732-747.
7. Akagi H, Nabae A, Atoh S. Control strategy of active power filters using multiple-voltage source PWM converters. IEEE Trans. Ind. App.1986; 22:460-465.

8. Tangtheerajaroonwong W, Hatada T, Wada K, Akagi H. Design and Performance of a Transformerless Shunt Hybrid Filter Integrated Into a Three-Phase Diode Rectifier. IEEE Trans. Power Electronics 2007; 22:1882-1889.
9. Srianthumrong S, Akagi H. A medium-voltage transformerless AC/DC power conversion system consisting of a diode rectifier and a shunt hybrid filter. IEEE Trans. Ind. App.2003; 39:874-882.
10. Srianthumrong S, Fujita H, Akagi H. Stability analysis of a series active filter integrated with a double-series diode rectifier," IEEE Trans. Power Electronics.2002; 17:117–124.
11. Lin B. R, Yang B. R, Tsai H. R. Analysis and operation of hybrid active filter for harmonic elimination. Electric Power Systems Research, 2002; 62: 191-200.
12. Dan S. G., Magureanu R, Asiminoaei L, Teodorescu R, Blaabjerg F. DSP control of line hybrid active filter", Proceedings of the IEEE International Symposium on Industrial Electronics, June 2005 Dubrovnik, Croatia2005. pp.1729-1734.
13. Na H, Jian W, Dianguo X. A Novel Shunt Hybrid Power Filter for Suppressing Harmonics. Proceedings of the IEEE International Symposium on Industrial Electronics, July 2006, Montreal, Canada 2006. pp.1155-1160.
14. Sarra M, Djazia K, Chaoui A, Krim F. Three-phase Active Power Filter with Proportional Integrator control. Journal of Electrical Systems, Special Issue 2009; 1: 79-84.
15. Chaoui A, Gaubert J. P, Krim F, Champenois G. IP controlled three-phase shunt active power filter for power improvement quality, Electric Power Components and Systems. 2007; 35: 1331-1344,
16. Benhabib M. C, Saadate S. A new robust experimentally validated phase locked loop for power electronic control. EPE journal, vol.15, no3, pp.36-48, August 2005.
17. Chaoui A, Gaubert J. P, Krim F. Experimental Evaluation of a Simple Robust Control for Active Power Filtering Under Unfavorable Conditions. European Conference on Power Electronics and Applications, EPE 2009, Sep. 2009, Barcelona, Spain.
18. Sarra M, Gaubert J. P, Chaoui A, Krim F. Experimental Validation of two Control Techniques Applied to a Three Phase Shunt Active Power Filter for Power Quality Improvement. International Review of Electrical Engineering Vol. 6. n. 6, pp. 2825-2836 (Special Issue), November 2011.
19. Sarra M, Gaubert J. P, *Chaoui A, Krim F.* Control Strategy of a Transformerless Three Phase Shunt Hybrid Power Filter using a robust PLL. IECON 2012. 38th Annual conference on IEEE Industrial Electronics society. 2012 Canada. pp.1258-1267.